forests

MDPI

Article

Moisture and Temperature Profiles of Heartwood *Pinus pinaster* Ait. Wood Specimens during Microwave Drying

Fernando Júnior Resende Mascarenhas [1,2,*], Rogério Manuel dos Santos Simões [3], Alfredo Manuel Pereira Geraldes Dias [1,2], André Luis Christoforo [4] and André Eduardo Palos Cunha [3]

[1] University of Coimbra, ISISE, ARISE, Department of Civil Engineering, Rua Luís Reis Santos—Pólo II, University of Coimbra (UC), 3030-788 Coimbra, Portugal; alfgdias@dec.uc.pt
[2] SerQ—Innovation and Competence Forest Centre, Rua J, No 9, Zona Industrial da Sertã, 6100-711 Sertã, Portugal
[3] Unit of Fiber Materials and Environmental Technologies (FibEnTech-UBI), Department of Chemistry, University Beira Interior (UBI), 6201-001 Covilhã, Portugal; rmss@ubi.pt (R.M.d.S.S.); aepcunha@gmail.com (A.E.P.C.)
[4] Department of Civil Engineering, Federal University of São Carlos (UFSCar), Rodovia Washington Luís (SP-310), Km 235, São Carlos 13565-905, Brazil; christoforoal@yahoo.com.br
* Correspondence: fer.jr.resende@hotmail.com

Abstract: Microwave (MW) drying of wood has gained popularity in the field of wood modification. The rise in temperature during MW drying leads to increased steam pressure, enhancing wood permeability but potentially decreasing mechanical properties. Understanding temperature and moisture behaviors during MW drying is crucial for its industrial application in wood drying. Therefore, this study aimed to characterize the temperature and moisture behaviors during MW drying of small Portuguese maritime pine (*Pinus pinaster* Aiton.) wood samples to support a wider use of this technology. The effects on water uptake and the compressive strength parallel to the grain were also investigated. The results indicated three distinct phases in the MW drying rates, with an average of 0.085% of water removed per second. Moreover, the temperature underwent three distinct stages: an initial rapid increase, a period of constant temperature, and a slight decrease until drying was complete. At the beginning of MW drying, the temperatures were below 100 °C, with average temperatures ranging from 126 to 145 °C. Specimens with lower initial moisture content had higher temperatures, and a positive correlation was found between initial moisture content and drying time. In contrast, negative correlations were found between the initial moisture content and average temperature, as well as average temperature and MW drying time. Additionally, the operating condition parameters used in MW drying of pine samples enhanced water impregnability by 65%, generating a slight reduction of 11% in compressive strength. It was also noticed that the initial moisture content did not impact MW-dried samples' water uptake or compressive strength. Finally, although small clear wood samples of maritime pine were utilized, the temperature and moisture patterns observed closely matched real-scale specimens. Thus, the findings corroborate a wide utilization of MW technology for wood drying, mainly demonstrating positive possibilities for structural-sized wood specimens.

Keywords: electromagnetic heating; initial moisture content; temperature characteristics; impregnability; compressive strength

check for updates

Citation: Mascarenhas, F.J.R.; Simões, R.M.d.S.; Dias, A.M.P.G.; Christoforo, A.L.; Cunha, A.E.P. Moisture and Temperature Profiles of Heartwood *Pinus pinaster* Ait. Wood Specimens during Microwave Drying. *Forests* **2024**, *15*, 944. https://doi.org/10.3390/f15060944

Academic Editors: Morwenna Spear and Miklós Bak

Received: 26 April 2024
Revised: 24 May 2024
Accepted: 28 May 2024
Published: 30 May 2024

Copyright: © 2024 by the authors. Licensee MDPI, Basel, Switzerland. This article is an open access article distributed under the terms and conditions of the Creative Commons Attribution (CC BY) license (https://creativecommons.org/licenses/by/4.0/).

1. Introduction

The limited permeability of many wood species presents challenges throughout the transformation process, including drying and impregnation. The conventional drying methods might have certain drawbacks, such as long drying times, substantial material losses, and expensive drying operations. Moreover, poor drying processes result in drying tensions and cell collapse, leading to defects and significant losses in the recovery of

sawn timber. Consequently, the timber industry continuously seeks methods to enhance wood permeability, reduce internal tensions, and prevent downgrading caused by drying errors [1].

Wood drying using electromagnetic waves as an energy source has gained popularity, particularly with the use of microwave (MW) energy, which is a promising technology in the field of wood modification [2]. The various benefits of this technology include high-quality drying combined with a fast process and significant improvements in porosity and permeability, which, for example, make it possible to solve the problem of wood species that are difficult to treat (impregnate) [3].

When considering the process of drying wood, it becomes essential to understand how water molecules are present within the wood, mainly because that topic has been investigated for decades [4]. They can exist in two distinct manners within the structure of the wood. One manner is free or capillary water, found within the capillaries, void spaces, cell lumen, and cavities. The interaction between free water and the wood takes place due to the surface forces. The second manner is known as bound water, in the cell wall, which is chemically combined with the chemical constituents of the wood, such as cellulose, hemicelluloses, and lignin. This combination primarily occurs through the formation of hydrogen bonds with the hydroxyl groups [5,6]. The theoretical stage at which all free water has been completely depleted and only bound water remains is called the fiber saturation point (FSP), which is inherently difficult to directly quantify since it depends on the wood species and the method used to measure it [5].

Regarding the drying process, the bound water is more difficult to be removed [5]. One of the reasons is that "the water molecules 'bound' in the first uni-molecular layer at the surface of the material are less rotationally free than the water in capillaries and cavities" [6]. In the process of MW drying, the entirety of the sample is permeated by electromagnetic waves, which facilitates the absorption of heat throughout the volume of the wet wood specimen [6,7].

Water molecules have polar configurations, which makes them prone to interact with the MW electromagnetic field [6,8]. In the presence of an alternating external electrical field, the molecule oscillates as it endeavors to align with the prevailing direction of the field [8]. Hence, microwave heating operates by converting electromagnetic energy into thermal energy locally. As a result, rapid heating occurs across the thickness of the material, accompanied by a reduction in thermal gradients. This volumetric heating process can effectively reduce drying times and conserve energy [7]. Du et al. also claim that the energy consumption savings in the MW drying process can be up to 50% [9].

Depending on the power supplied by the MW device, the energy absorbed, and the duration of the drying process, the temperature within the wood can experience a rapid rise, leading to the generation of significant steam pressure [2,3,10]. The potential of microwave electromagnetic energy to rapidly remove moisture from wood [11] results from the formation of steam within the wood, which can displace capillary liquid water and provide a favorable driving force for mass transfer. The total pressure (mainly derived by the water vapor) difference between the different positions inside the wood and on the inside and outside generates tension that can damage the more vulnerable cell structures, such as pit membranes and ray parenchyma cells.

As a consequence, this phenomenon leads to the emergence of novel pathways through which liquids can flow within the wood. As a result, there is an overall increase in the wood's porosity (and therefore permeability). However, if the MW parameters are not properly adjusted, for instance, elevate powers, the MW drying process may also negatively affect strength and stiffness [3,12,13], which is not desirable, especially if the wood dried in the MW is to be used for structural purposes later on.

Xiao et al. [14] explain that the extent of structural impairment is ascertained by the magnitude of internal pressure within the wood element during the process of microwave drying. Therefore, the internal water pressure assumes a pivotal function in determining the extent of damage to the microstructure [14]. As the internal water pressure generated during

MW drying is directly linked to temperature, it is expected that a balance between the drying rate and wood damage should be established by controlling the internal temperature and, consequently, the pressure generated by the MW drying. In other words, knowing the MW drying rates and the profile of internal temperatures throughout the MW drying process are crucial.

In the literature, temperature measurements were made in different ways and positions inside and outside the wood samples. Due to operational issues, in some works, the temperatures of the wood specimens were analyzed outside the oven after each MW drying cycle [15–17]. Other authors [14,18,19], in turn, used a continuous measurement of the temperature inside the samples during the MW drying, which seems to be the most appropriate. In addition, most of the works presented in the literature that investigated the temperature in MW-dried samples used wood samples containing only sapwood, or both stem parts (with no differentiation between the two within the same wood specimen).

Acknowledging that the research works in the literature have demonstrated that the wood species and the stem part are important parameters that influence MW drying [2,20], there are still scarce investigations about the moisture and temperature profiles during MW drying of one of the most used wood species in the construction, civil engineering, and furniture industry in southwestern Europe, the native maritime pine (*Pinus pinaster* Ait.) [21]. Besides those different uses, pine is also recognized as an ecologically versatile wood species [22].

Hence, based on the benefits of MW drying, the importance of temperature profiles throughout the MW drying process, and the economic and environmental noteworthiness of maritime pine wood species, the objective of this study was to foster the use of MW technology to dry wood by analyzing the interior temperature profile of small clear specimens of Portuguese maritime pine containing only heartwood during the MW drying, examining the drying and temperature behavior over the MW drying time and the reduction of the amount of water in the samples, and investigating the changes in the water impregnability and compressive strength.

The studied wood samples had different initial moisture contents (IMC), and the influence of this parameter on the drying rates, temperature profile, water uptake, and compressive strength parallel to the grain was explored. In addition, the drying and temperature profiles of the small clear maritime pine wood samples studied in this work were also compared with studies that investigated MW drying with full-scale wood elements (structural-sized samples).

Although the literature indicates that sapwood and heartwood react differently when dried [23], studies have demonstrated that heartwood is more severely affected by MW drying in terms of microstructural modifications than sapwood [2]. Also, different authors have focused their studies only on one of the wood stem parts to properly understand the effects of MW energy, either in sapwood or heartwood. Thus, it was chosen to work with maritime pine samples containing only heartwood since this wood stem part is usually much less permeable than sapwood [24], and it is extremely difficult to be impregnated with preservative products [25,26]. Hansmann et al. [27] explain that in a specific species, the permeability is typically higher in sapwood compared with heartwood due to the latter's increased level of pit aspiration and encrustation with extractives.

2. Experimental

2.1. Material

A total of 84 small clear Portuguese maritime pine specimens containing only heartwood, with an average oven-dry density of 697 $\pm$ 43 kg/m^3, were prepared from commercial boards, with dimensions 10 mm $\times$ 10 mm $\times$ 200 mm (Radial $\times$ Tangential $\times$ Longitudinal), and they were MW-dried (Figure 1). Another 21 samples of the same dimensions were prepared and dried using conventional methods (without MW drying), and they were referenced as the control group. These control samples were used in the water impregnability and compressive strength tests.

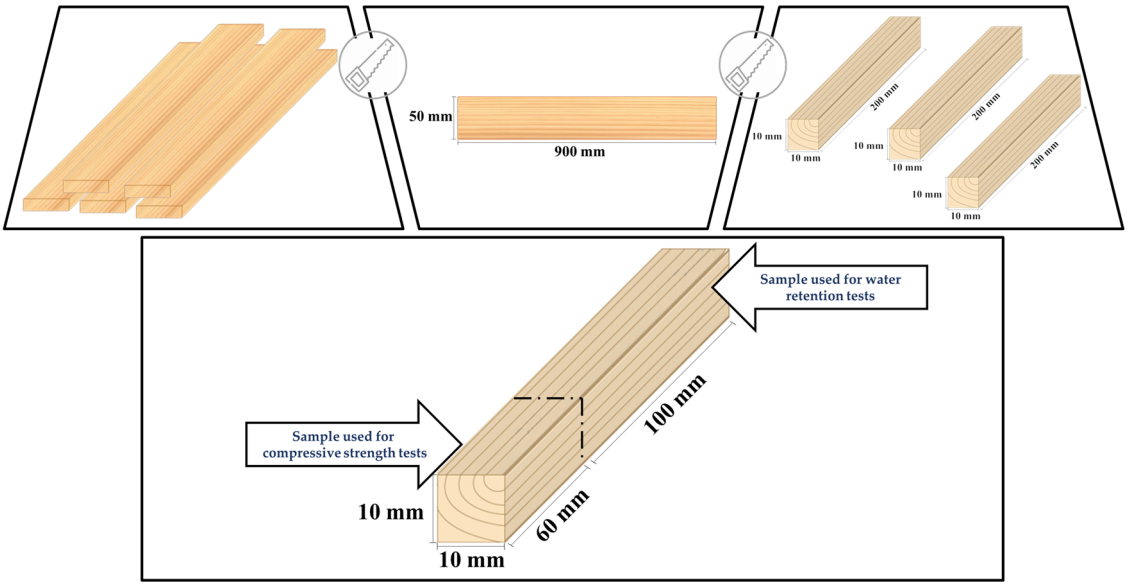

Figure 1. The preparation of wood samples. The dashed line represents the wood section in which the cut was done.

Following the same approach that Kol and Çayır [11] used in their work, 16 other extra wood samples were randomly selected from the same commercial boards and cut in the dimensions of 10 mm × 10 mm × 200 mm to determine their oven-dry mass. Using the average oven-dry mass of these samples, the IMC of the 84 samples used in the MW drying process and their moisture content (MC) evolution during the MW drying were assessed. The MC was determined according to ISO 13061-1 [28]. The wood specimens subjected to the MW drying were grouped based on their IMCs, i.e., wood samples with similar IMCs were placed in the same group, as shown in Table 1. The IMCs of the four MW-dried wood groups were statistically different.

Table 1. Samples' average IMC and quantity.

Group	IMC (%)	Number of Samples
1	63.39 (2.65) ^{D}	21
2	75.50 (5.20) ^{C}	21
3	81.12 (3.56) ^{B}	21
4	92.19 (2.70) ^{A}	21

The numbers in parentheses are the standard deviation. Values associated with different letters in Tukey tests show significant differences with a *p*-value of 0.05.

Furthermore, what can be observed in the literature is that in most studies involving MW drying, small clear wood samples are used [2]. Small clear samples have certain advantages, such as being easier to work with, more economically attractive in terms of material, resources, and laboratory space required for testing, and allowing different tests and analyses to be carried out before moving on to full-scale structural parts. The British Standard BS 373:1957 [29] states that the results from the tests might also be used to assess the impact of different treatments on strength, density, and other properties and aid in creating design equations for structural timbers.

2.2. Microwave Drying

MW dryings were performed using a conventional domestic MW device measuring 200 mm × 300 mm × 300 mm (inner chamber), with a frequency of 2.45 GHz, maximum output power of 800 W, and a specific applied power of 5714 kW/m^3, per MW drying

cycle. A homogenous wave distribution inside the chamber was expected through a fan at the top of the MW device, through which the waves come out, which contributed to a better distribution of the waves inside the equipment's cavity. The MW oven also has a turntable, which contributes significantly to the homogeneous distribution of the waves. As presented in Table 1, the wood specimens were divided into four groups, and each group of 21 samples was divided into three sub-groups of seven samples (Figure 2). The seven samples of each sub-group were placed together in the MW to be dried simultaneously, and they were dried until they achieved an average of 12% ± 2% final moisture content.

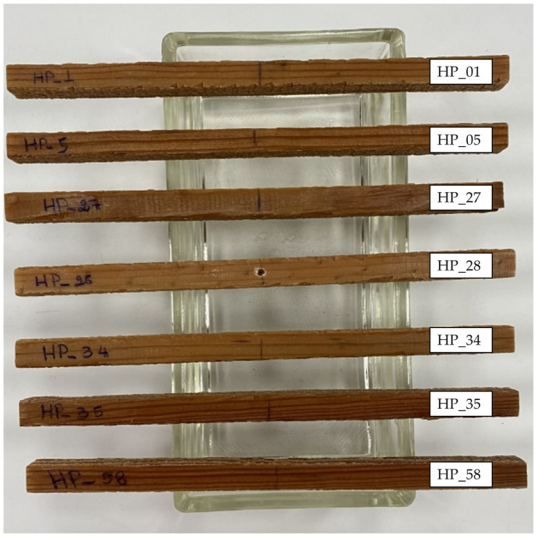

Figure 2. Wood samples dried together. "HP" in the figure stands for "heartwood pine".

The drying program used in this work was based on previous tests and also followed what Mascarenhas et al. [30] adopted in their work, with 30 s inside the MW oven (wood samples continuously exposed to MW), followed by a 30 s cooling interval (Figure 3).

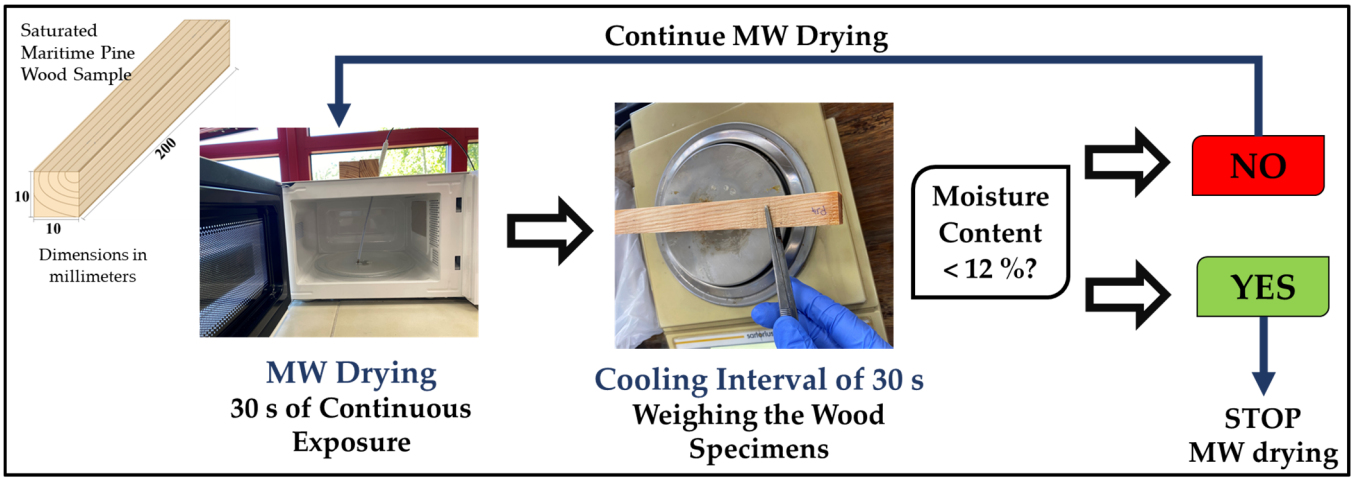

Figure 3. MW drying process program.

The MW applied energy intensity, E, was calculated using Equation (1) [11]:

$$E = \frac{P \cdot t}{V \cdot 10^6} \quad (1)$$

where E is the energy supplied during the MW process, in MJ/m^3; P is the MW power supplied (W); V is the volume of wood specimen, in m^3; and t is the drying time, in s.

Adopting the same procedure that other authors used [11,31], the weight percentage loss (*WPL*) and relative water loss (*RWL*) were calculated using Equations (2) and (3):

$$WPL = \frac{m_2 - m_1}{m_{od}} \times 100 \quad (2)$$

where m_2 is the weight of the specimen before MW drying in g; m_1 is the weight of the specimen after MW drying, in g; and m_{od} is the oven-dry weight of the specimen, in g.

$$RWL = \frac{WPL}{IMC} \quad (3)$$

The MW drying and heating rates were calculated using the following Equations (4) and (5), respectively:

$$dr = \frac{MC_t - MC_{t+\Delta t}}{\Delta t} \quad (4)$$

$$hr = \frac{T_{t+\Delta t} - T_t}{\Delta t} \quad (5)$$

where dr is the drying rate, in %/s; Δt is the time interval of drying, in s; hr is the heating rate, in °C/s; and T is the measured temperature in wood, in °C.

2.3. Temperature Measurements

A Heidolph EKT 3001 thermometer was used to measure the temperature inside the wood samples (5 mm deep at the center and middle) (Figure 4). The position was chosen based on previous works from the literature [14,18] and because the MW energy is provided in order to produce heat internally within the solid wood, which then moves to the outer surface [32]. The temperature measurements were made during the entire drying process and recorded at intervals of 5 s during each 30 s drying cycle inside the MW device. The measuring probe was removed while weighing the specimens, and a silicone seal was placed in the hole to avoid excessive evaporation.

Figure 4. Temperature measurement.

Based on the temperature measurements, the water saturation pressure was calculated according to Equation (6) [33], assuming liquid/vapor equilibrium:

$$P_s = -0.59 + 0.2846 \cdot T - 0.00867 \cdot T^2 + 0.000159 \cdot T^3 \quad (6)$$

where P_s is the water saturation pressure at a given temperature, in kPa; and T is the measured temperature in wood, in °C.

2.4. Water Uptake and Compressive Strength Parallel to the Grain Tests

To better investigate the effects of MW drying on wood samples, i.e., possible impacts on the microstructure and mechanical integrity of the wood samples, two tests were conducted to analyze the modifications: (1) the impregnability to distilled water and (2) the compressive strength parallel to the grain ($f_{c,0}$). Both tests were carried out on specimens dried with MW and those without MW (control).

The impregnability tests were performed to indirectly verify if the treatability of the heartwood of maritime pinewood samples changed. Then, wood samples measuring 10 mm × 10 mm × 100 mm were placed in an autoclave filled with distilled water, and a pressure of 600 kPa was applied for 30 min. Based on this, the water uptake, WU, was calculated using Equation (7):

$$WU = \frac{m_{ai} - m_{bi}}{m_{od}} \times 100 \quad (7)$$

where m_{ai} is the weight of the specimen after water impregnation, in g; m_{bi} is the weight of the specimen before impregnation, in g; and m_{od} is the oven-dry weight of the specimen, in g.

Besides that, tests were carried out to determine the compressive strength. Compressive strength is one of the most important mechanical properties of wood [34–38], mainly because modified wood with reduced compression strength might have restricted use [35]. Following the recommendations of Standard EN 408 [39], as performed by Hermoso and Vega [40], the tests to determine $f_{c,0}$ were carried out on test pieces measuring 10 mm × 10 mm × 60 mm. Subsequently, the results were adjusted to 12% moisture content, resulting in the compressive strength parallel to the grain at 12% moisture content ($f_{c,0,12\%}$).

2.5. Analysis of the Results

To assess the significant differences between the variables studied in this work, the classical analysis of variance (ANOVA) was employed at a significance level of 5% associated with the Tukey test. According to ANOVA and Tukey, in the event that the p-values are lower than the designated significance level (p-value < 0.05), it is plausible to assert that the analysis holds statistical significance. Moreover, when conducting a statistical analysis involving 2–9 groups with ANOVA methodology, it is necessary that the minimum sample size for each group is 15 [41]. For the current study, four groups (MW drying and temperature profiles) and five groups (water uptake and compressive strength) were utilized, with each group consisting of 21 specimens.

Pearson's correlation coefficient (r) was used to measure linear relationships between (1) MW drying time and IMC, (2) average temperature of the samples and IMC, and (3) average temperature of the samples and MW drying time. In addition, regression models, adjusted by the least squares method, were applied to determine the equations to estimate (1) MW drying time as a function of the IMC, (2) average internal temperature of the samples as a function of the IMC, and (3) average internal temperature of the samples as a function of the MW drying time. The R-squared (R^2) was used to measure the proximity of the data points to the regression line that has been fitted. All statistical analyses were conducted utilizing the Minitab 18 software (version 2017) [41].

3. Results and Discussion

3.1. MW Drying Profile

The time profile of the average MC of the four MW wood-dried groups is presented in Figure 5. Despite the difference in IMC, the MC profiles over the MW drying time were very similar. The findings using small clear maritime pine wood specimens were generally consistent with Sethy et al. [17], Xiao et al. [14], and Weng et al. [42], who utilized the MW technology to dry structural-sized (industrial scale) samples of different wood species.

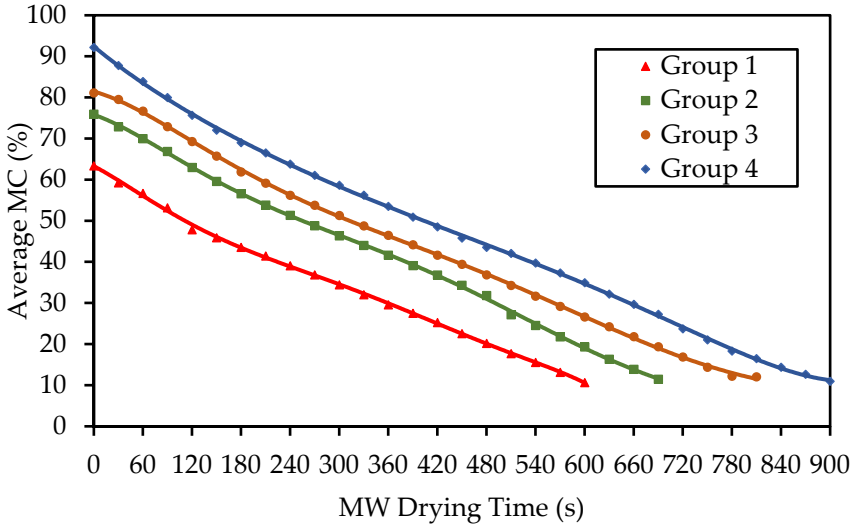

Figure 5. Average moisture content along the MW drying process.

The total MW drying time (total time the specimens were exposed to MW energy), the average initial and final moisture contents, the average MW drying rates, the average MW applied energy, the WPL, and RWL are shown in Table 2. The average MW energy supplied to the wood samples increased as the IMC increased. Additionally, higher volume of water requires more time for removal from the wood samples, directly impacting the total drying time.

Table 2. MW drying characteristics.

Group [1]	Average IMC (%)	Average Final MC (%)	Total MW Drying Time (s) [2]	Average MW Drying Rates (%/s)	Average *E* (MJ/m^3)	WPL (MJ/m^3)	RWL
1	63.39 (2.97)	10.66 (0.44)	600 ^{D}	0.082 (0.033) ^{A}	3429 (74) ^{D}	52.73 (1.14) ^{D}	83.18 (1.80) ^{A}
2	75.50 (5.20)	11.48 (0.66)	690 ^{C}	0.089 (0.023) ^{A}	3943 (276) ^{C}	64.02 (4.48) ^{C}	84.79 (5.94) ^{A}
3	81.12 (3.56)	11.46 (0.55)	810 ^{B}	0.085 (0.021) ^{A}	4629 (258) ^{B}	69.66 (3.88) ^{B}	85.87 (4.79) ^{A}
4	92.19 (2.70)	10.96 (0.57)	900 ^{A}	0.082 (0.027) ^{A}	5143 (159) ^{A}	81.23 (2.51) ^{A}	88.11 (2.72) ^{A}

[1] All four groups had 21 wood specimens each. [2] MW drying time represents the total time the samples remained inside the MW device, excluding the cooling intervals. The numbers in parentheses are the standard deviation. Values associated with different letters in Tukey tests show significant differences with a *p*-value of 0.05 within the same variable analyzed.

Despite the difference in IMC of the four groups of samples, the average drying rates for groups 1, 2, 3, and 4 were statistically equivalent (confidence interval, CI, of 95%) and equal to 0.082, 0.089, 0.085, and 0.082 percentage of removed water per second (%/s), respectively. Leiker and Adamska [43] measured MW drying rates up to 0.075%/s for *Fagus sylvatica* and *Picea abies*. Ouertani et al. [18] MW-dried *Pinus banksiana* with 12 mm thickness with MW power ranging from 300 to 1000 W, and the average MW drying rates varied from 0.017 to 0.133%/s. A linear interpolation of these results [18] for 800 W, the same used in this work, shows that the drying rate was 0.093%/s, which is within the values presented here. An analysis with further details was carried out in the following section, where the MW drying rate results were correlated with the temperature profile.

The WPL values ranged from 53 to 81%, and the RWL from 83 to 88%. Kol and Çayir [11] had WPL values ranging from 47 to 50%. Additionally, the amount of energy supplied to the maritime pine specimens to remove 1% of the water was 65.0, 61.6, 66.5, and 63.3 MJ/m^3, respectively, for wood groups 1, 2, 3, and 4. For instance, MW drying structural-sized samples of *Eucalyptus obliqua* and *Pinus radiata* heartwood, Torgovnikov and Vinden [13] indicated that 66 and 21 MJ/m^3 were applied to dry 1% of the water of each wood species, respectively, evidencing the dielectric properties of wood [44].

3.2. Temperature Profile during MW Drying

In order to analyze the evolution of the temperature inside the specimen at each 30 s MW drying cycle, the temperature was measured every 5 s (5, 10, 15, 20, 25, and 30 s). Figure 6a shows the average temperature profile over the MW drying time for group 1. In addition, the temperature profile at three different moments of the MW drying process during 30 s of continuous exposure time is presented in Figure 6b–d. Whether at the beginning, middle, or end of the drying process, the temperature peaks can be noticed at the end of each 30 s cycle. Those peaks may be responsible for causing the most significant damage to the microstructure of the wood due to the high pressures generated in the interior (as shown further ahead), which, on the other hand, leads to increased porosity and, consequently, permeability. The degree of structural alterations or even damage is typically determined by these temperature peaks, which are a function of the energy intensity of the MW drying, which, together with MW drying time, are important variables in the change in anatomical structure [2].

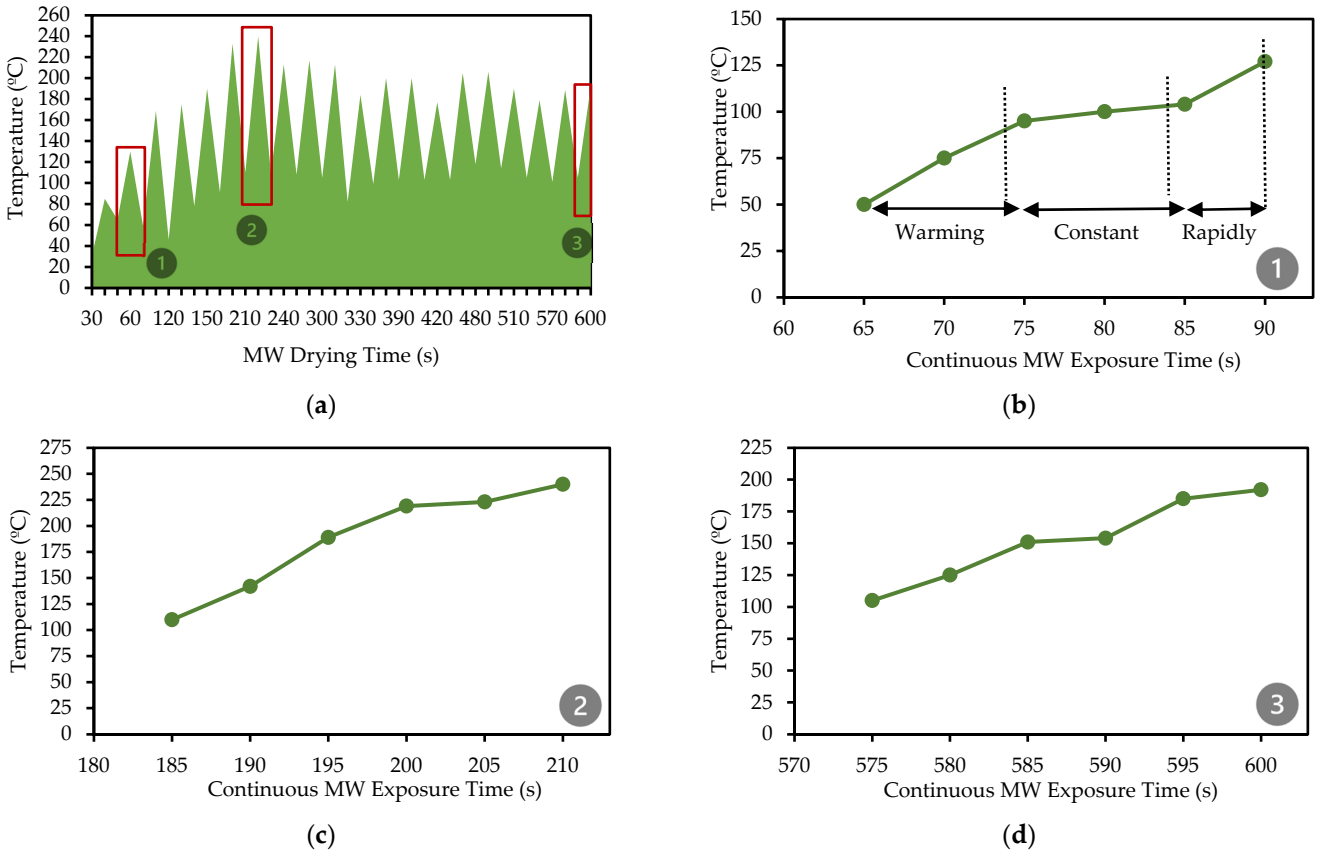

Figure 6. Temperature behavior (average) in each interval of measurement for group 1 (**a**) during the complete drying process, with a focus on the (**b**) beginning, (**c**) middle, and (**d**) ending of the drying process. Continuous MW Exposure Time represents the time the wood samples were inside the MW device.

Despite the reduced dimensions of the cross-section of the samples, these findings suggest that the cooling intervals of 30 s (outside the MW oven) were necessary and effective to avoid prolonged exposure of the wood specimens to MW energy. Hence, two main consequences could arise if the wood specimens were continuously exposed to these MW drying conditions (for too long, without the cooling intervals). First, extremely high pressure could be generated due to the extremely high temperatures, leading to excessive damage to the wood's microstructure and the appearance of cracks. When analyzing

the surface of the pine wood specimens dried in the MW, no visible drying defects were observed, which is due to the aforementioned factors.

Second, the wood samples could burn, leading to the charring of the wood. A similar approach was used by other authors [45], who dried *Abies alba* L. wood samples for 30 to 60 s and made cooling intervals of 60 to 120 s. Oloyede and Groombridge [8] also explain that each consecutive exposure enables a deeper penetration level. Each specimen's weight was carefully measured with a scale and recorded for weight control purposes to follow the moisture content decrease along the drying process. Thus, a non-continuous MW drying process was carried out.

The drying time interval of 60 to 90 s, which is shown in Figure 6b, has three behavior patterns: a warming period, constant temperature around the water's normal boiling point, and a rapidly rising temperature with heating rates of 3.33, 0.90 and 4.60 °C/s, respectively for each phase. Although the drying in the MW carried out in this work was not continuous, as is more common for structural-sized pieces, the beginning of the MW drying process showed a profile similar to that found by the authors [14], using a continuous tunnel MW equipment and *Pinus sylvestris* L. var. *mongolica* Litv. samples of 480 mm (longitudinal) × 980 mm (tangential) × 930 mm (radial).

In Figure 6c, we have the average temperatures during the 30 s measured in the middle of the drying process (210 of total MW drying time), when the highest temperatures were achieved, with a heating rate of 5.20 °C/s and a drying rate of 0.10%/s. Finally, Figure 6d shows the temperatures during the final 30 s drying interval (total MW drying time equal to 600 s), with a heating rate of 3.48 °C/s and a drying rate of 0.08%/s.

The temperature profiles of the MW-dried samples for each group are shown in Figure 7. By analyzing the average inside-temperature profile along the entire MW drying process, it is possible to identify three distinct stages. Stage (1) a rapid increase in temperature (heating-up period), (2) a continuous period of relatively constant temperature, and (3) a decrease in temperature by the end of the drying process. By studying the MW drying in *Pinus sylvestris* wood samples, Hansson and Antti [46] obtained similar temperature profiles for Scots pine (*Pinus sylvestris*).

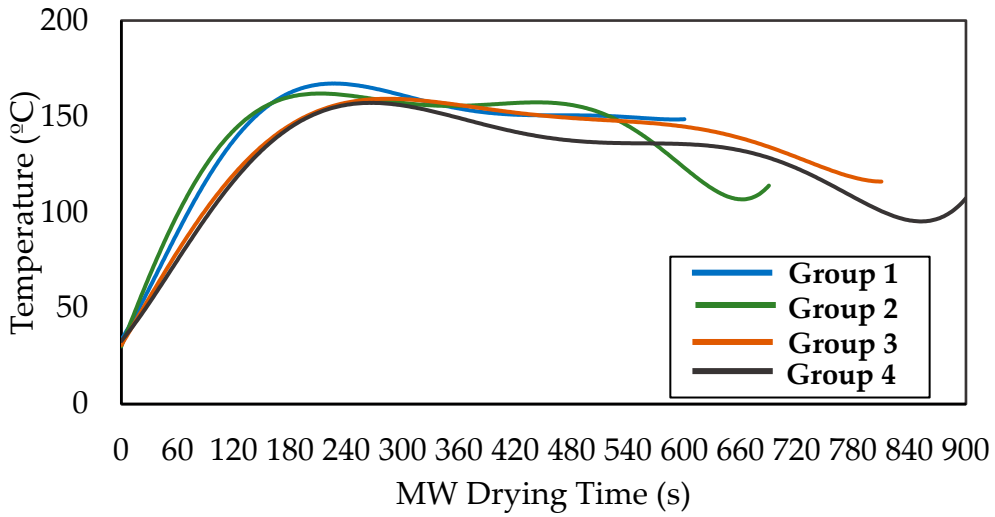

Figure 7. Average temperature over the MW drying process of groups 1, 2, 3, and 4.

Furthermore, the average temperature inside the samples remained over 100 °C for most of the MW drying time. Only at the beginning of the MW drying they were less than 100 °C, which ties well with previous studies developed by Vongpradubchai and Rattanadecho [47]. The rapid increase in temperature identified in the first couple minutes of the MW drying process demonstrates the volumetric heating in MW drying, which causes a fast transfer of energy throughout the wet wood sample. Internal evaporation and a rise in the total pressure might occur within the pores as the wet material's temperature

approaches the liquid's boiling point [6,48]. In addition, the initial rise in temperature observed during the heating-up phase signifies the peak level of MW power absorption by the wood. In this stage, wood with higher moisture content absorbs a greater amount of energy compared with dry wood towards the completion of the drying [18].

The data presented in Table 3 shows that there is a significant difference in the temperature profiles of the samples with the lowest and the highest initial moisture content, particularly at the beginning of the drying process. The samples from groups 1, 2, 3, and 4 took approximately 50, 55, 80, and 105 s, respectively, to reach 100 °C for the first time. When looking at the results of different wood groups, from the smallest to the highest IMC, the average temperatures in the first 5 s within the cycle remained below 100 °C more frequently as the initial water content increased. For instance, from the temperatures measured in the first 5 s of each cycle, the percentage that was equal to or less than 100 °C represented 42% for group 1 (IMC = 63%), 61% for group 2 (IMC = 76%), 89% for group 3 (IMC = 81%), and 100% for group 4 (IMC = 92%). Xiao et al. [14] explain that under similar conditions of MW drying, a higher amount of energy was required to raise temperatures when the moisture level was elevated, resulting in a reduction of the drying rate and maximum measured temperature.

Table 3. Average measured temperatures and estimated pressure inside the wood samples.

Group	Average Temperature (°C)	Time to Achieve 100 °C (s)	Maximum Temperature (°C)	Average Pressure (kPa)	Estimated Maximum Pressure (kPa)
1	145	50 (after 1st cooling interval)	240	331	1766
2	140	55 (after 1st cooling interval)	236	291	1681
3	136	80 (after 2nd cooling interval)	232	282	1584
4	126	105 (after 3rd cooling interval)	222	215	1375

Also, based on Table 3, two contributions to these results can be drawn. First, the samples in the studied groups with higher IMCs had more free water in their cell spaces, so the MW energy was dissipated into more water. The temperature increase was slower than in the case of wood with lower IMCs. Therefore, the majority of them stayed in the liquid condition for more time; more energy was used to heat and vaporize the water, and no significant increase in temperature occurred. Second, softwoods are permeable due to pit pairs connecting tracheid lumens, allowing flow when the vapor pressure is generated within the wood above the fiber saturation point and at high temperatures [32], the wood samples from the groups with higher quantities of IMC might indicate that those samples had the interior structure more "open", with, for example, the bordered pit not aspirated, which ended up letting steam out [4,49], and, with that, the temperature increase is more moderate. The experimental data did not enable us to establish the relative importance of these two mechanisms.

The average water saturation pressure estimated based on Eq. 6 of the small clear wood samples ranged from 215 to 331 kPa (Table 3), which is within the stem pressure measured by Torgovnikov and Vinden [13], who MW-died structural-sized wood in a continuous MW device. The authors measured values up to 600 kPa and, for these values, reported severe wood microstructures and cell damage corresponding to/associated with high losses in mechanical properties.

Figure 8 shows the average drying rates of the four groups. Comparing the drying rate profiles with the corresponding temperature profile (Figure 7), an initial boost in drying rate is observed for the four groups. This boost can be due to what some authors call liquid

movement [6]. Similar drying rate behaviors were observed for other wood species, *Pinus banksiana* [18], oriented strand board made of pine [9], and *Eucalyptus globulus* [30].

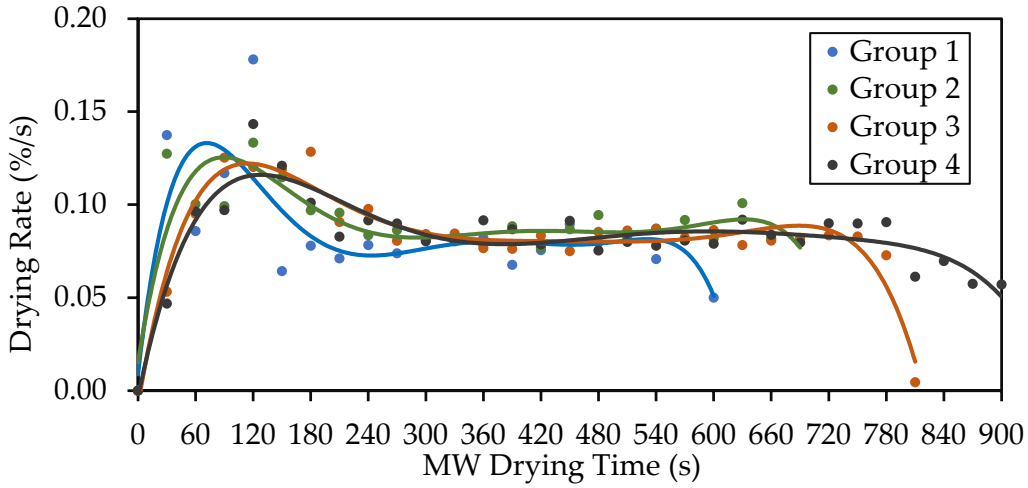

Figure 8. MW drying rate behavior over the MW drying process for the four wood groups.

When observing the drying rate behavior over the reduction of MC (Figure 9) of the non-continuous drying process in the MW of small specimens of maritime pine, it can be seen that there are three stages involving the drying rate: (1) a liquid movement period, (2) a constant drying rate, and (3) a falling drying rate period. These same stages were observed when a continuous MW drying process was carried out with large-scale samples [6]. The average drying rates during the heating-up period (which coincides with the liquid movement stage) for groups 1, 2, 3, and 4 were 0.094, 0.096, 0.091, and 0.086%/s, respectively. The heating rates in the same period were 4.08, 3.85, 3.53, and 3.52 °C/s for groups 1, 2, 3, and 4, respectively. The extremely high drying rates in the last part of the heating-up period can be related to the water's movement (expulsion) in a liquid state due to the high pressure developed inside the wood. Other authors reported this phenomenon as filtrational flow caused by the total pressure gradient [6].

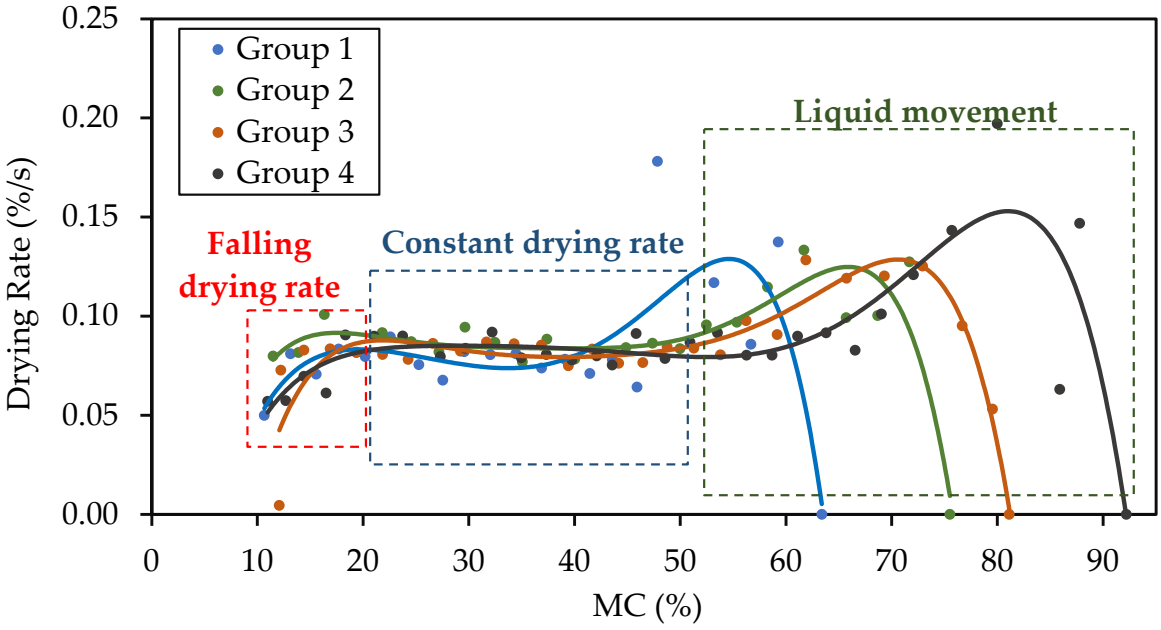

Figure 9. MW drying rates as a function of MC (%) for the four groups.

Also analyzing Figure 9, it can be seen that the constant drying rate started at different moments because of their different IMCs. In addition, the duration of the constant drying rate lasted longer in groups with higher initial water content. This might have happened because the improved moisture flow to the surface was superior "than the additional moisture evaporated at the surface due to the heat conducted from the wet" wood [6].

According to Metaxas and Meredith [6], during the stage of constant drying rate, the moisture content is quite high, and evaporation from the surface will proceed at a steady pace as long as the ambient circumstances stay constant. The authors [6] also point out that the moisture moves from the interior of the wood to the surface by capillary forces to replace the evaporated water required for the constant drying rate period.

This part of the drying process demonstrates the advantage of MW wood drying. Zielonka and Dolowy [15] explain that in traditional drying methods, the movement of water from the inner layers to the outer surface of the wood is decreased. However, because in MW drying, the energy is effectively transmitted to the water molecules present in the wood samples, it becomes feasible to sustain a suitable flow of moisture towards the surface where evaporation occurs [15,16]. In other words, the constant drying rate period lasts longer, and as the moisture content of the wood decreases below a critical point, the MW drying rate decreases progressively, limited by the decreased amount of water that migrates from the interior of the wood to its surface [6].

Thus, we have the last part of the drying process, the falling drying rate period. With the decrease in moisture levels, the evaporation rate decreased progressively, restricted by the reduction of water migration from the core of the solid to its surface. As soon as the wood sample became drier, a continuous introduction of air pockets made it difficult for the liquids to flow from the interior to the surface. Hence, the drying started to be impeded because the water in the pores' menisci dropped below the evaporating surface [6].

As the drying time increases, the free water decreases, leaving only the bound water, and removing the bound water in wood is more difficult because this residual water absorbs little energy [6,50,51] since it is strongly bound with polar groups and less rotationally free than free water [52]. In fact, when analyzing the drying rate over the moisture content reduction (Figure 9), it was noticed that from the IMC until a MC of about 24% (theoretical FSP for maritime pine [53]), the average drying rates of the four wood groups were greater than the average drying rates from that point to the ending of MW drying. Weng et al. [42] identified the same pattern in MW-dried structural-sized *Cunninghamia lanceolata* (Lamb.) Hook wood elements, where the drying rates with MC higher than the FSP were approximately 65% greater compared with when the MC is smaller than the FSP.

The temperature also started to decrease gradually by the end of the constant drying rate period and the beginning of the falling period, which is more evident in groups with higher IMC (Figure 10). One possible reason is the increase in wood permeability reached at the maximum temperature and pressure inside the structure, which facilitates the water vapor transfer to the outside and corresponding water evaporation inside, which provokes a temperature decrease inside the wood, where the sensor is located. The temperature reduction by the decrease of water vapor in contact with the temperature probe cannot be discarded. The maximum temperatures were reached at moisture contents of 41.44 (MC ratio of 0.65), 55.35 (MC ratio of 0.73), 59.16 (MC ratio of 0.73), and 66.54% (MC ratio of 0.73) for groups 1, 2, 3 and 4, respectively.

It was also observed that by the end of the MW drying process, the temperatures of the wood samples were, on average, approximately 150, 120, 115, and 105 °C for groups 1, 2, 3, and 4, respectively. Even though the temperatures were lower than the values measured in previous moments of drying, they were still high and above 100 °C, which could indicate a risk of overheating and charring the wood samples.

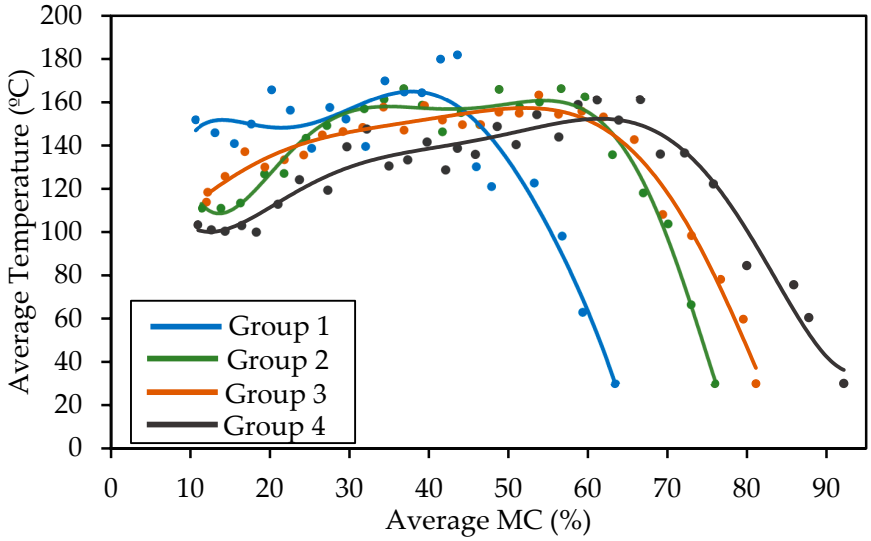

Figure 10. Average temperature behavior along with MC reduction for the four wood groups.

Finally, correlation analyses were used to corroborate what was previously presented and discussed. Figure 11 shows Pearson's correlation coefficient *r* and the *p*-values for the four wood groups. First, all the correlations were high and significant (*p*-value < 0.05). When analyzing the IMC and MW drying time (Figure 11a), there is a positive-strong correlation, 0.908, very close to 1. The higher the IMC, the more time is required to dry wood samples at the same power input, as expected.

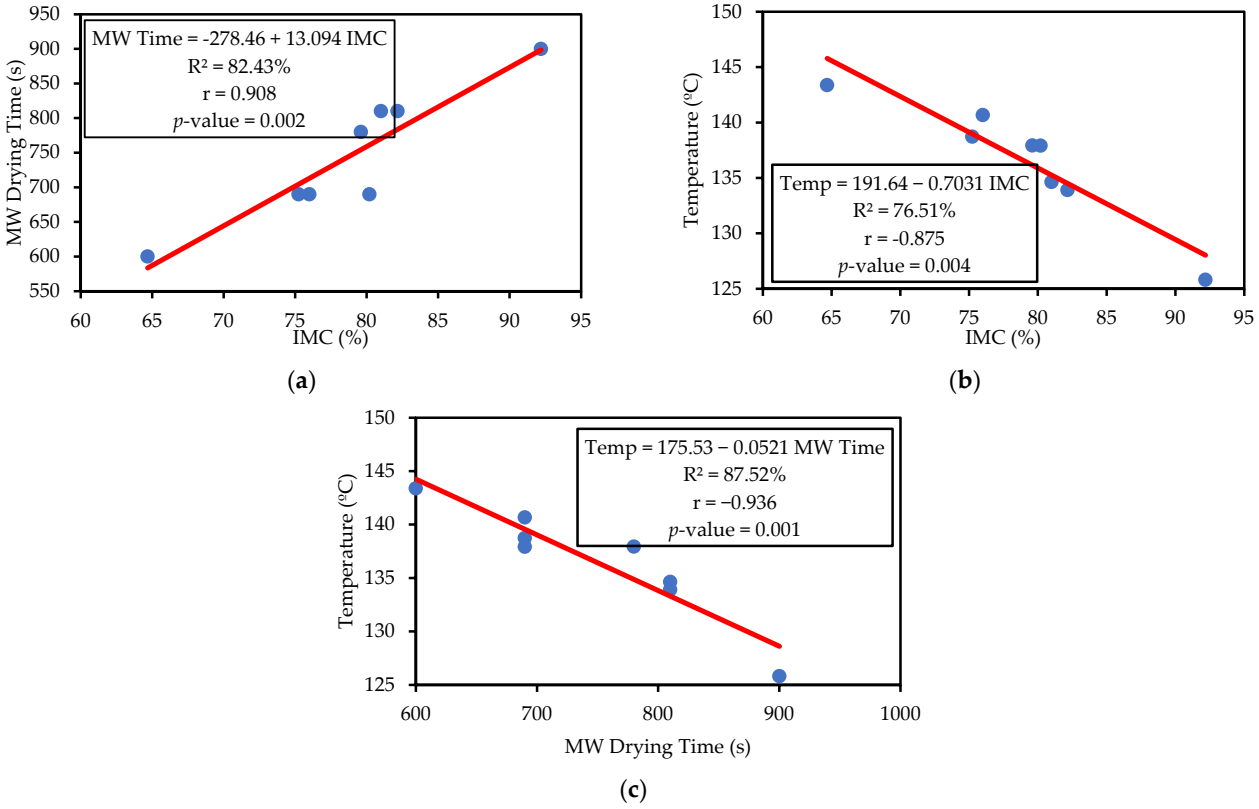

Figure 11. Correlation analysis: (**a**) MW Time and IMC, (**b**) Temperature and IMC and (**c**) Temperature and MW Time. Temp = average temperature; IMC = initial moisture content; MW Time = total MW drying time.

When analyzing the relationship between IMC and the temperature (Figure 11b), a negative-strong correlation of −0.875 indicated that the higher the IMC, the smaller the average temperature measured inside the sample. When evaluating the average temperature and MW drying time (Figure 11c), a negative-strong correlation of −0.936 indicates that the higher the MW drying time, the smaller the wood's internal average temperature. It is important to state that the MW drying time depends on the MW power and IMC of the wood samples. This is due to the fact that longer time is linked to higher IMC, which in turn leads to lower temperatures. This hypothesis is valid when MW power is a limiting factor.

In addition, by evaluating the equations presented in Figure 11, it is possible to notice that besides the elevated Pearson correlation coefficients, the high R^2 (from 75 to 87%) indicates that the three equations adequately estimate their respective variables. It is important to highlight that the idea of establishing equations to predict the total MW drying time and the average temperature has as objectives to plan better and organize the experimental drying campaigns, which can result in time saving and even material savings. Thus, it is possible to estimate both parameters before the drying process starts within the range of values analyzed here and with species with a density similar to the species studied in this work.

3.3. Evaluation of the Water Impregnability and Compressive Strength

The water uptake (WU) of the four wood groups and control samples is presented in Figure 12. The WU of MW-dried pine samples increased from 51 to 65% compared with control samples. Although the measurement of permeability was not conducted directly for the wood samples (both control and MW-dried) due to the existence of specialized techniques for such measurements, the observed enhancement in water uptake in the MW-dried samples in comparison with the control one could potentially suggest an elevation in their permeability levels.

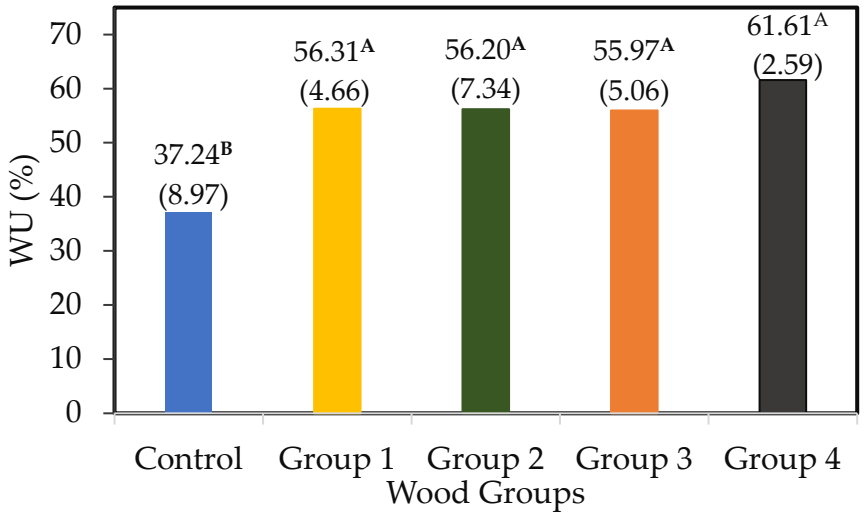

Figure 12. Average water uptake of the four wood groups. The numbers in parentheses are the standard deviation. Values associated with different letters in Tukey tests show significant differences with a *p*-value of 0.05.

He et al. [54] employed a comparable method in their study, utilizing water uptake measurements to indirectly assess the changes in the permeability of *Cunninghamia lanceolata* wood following MW drying on real-scale wood elements. Our results align with those from the authors [54] since they measured the retention of control samples of approximately 34%, and the MW-dried ones ranged from 44 to 77%.

The IMC was not a decisive factor in the WU since the four MW-dried groups had statistically equivalent WU values. Wang et al. [55] MW-died *Pinus sylvestris* var. mongolica Litv with different IMCs in real scale, and they observed that while the samples with an

IMC of 40% had no significant alteration in the cell wall morphology, and the cell structures remained unchanged, the cell wall structure of wood samples with an IMC of 20% exhibited the most severe modification.

The results showed that the peak temperatures measured on the pine specimens were probably not extreme. However, even so, they may have been high enough for the vapor pressure generated to lead to an increase in the impregnability of these samples. Hence, the rupture of weak ray cells might have created pathways that facilitate the transport of liquids, leading to enhanced permeability in the transverse direction when subjected to MW drying [13,23,42].

The compressive strength parallel to the grain was also measured (Figure 13). It is possible to conclude that despite slight reductions of 8 to 13% in the compressive strength parallel to the grain at 12% moisture content ($f_{c,0,12\%}$) of MW-dried samples compared with the control ones, the values of all wood groups were statistically equivalent. MW-drying small clear *Quercus pyrenaica* Wild wood samples, Machado [56] identified reductions in the compressive strength of 10 and 20%. Balboni et al. [57] measured reductions of approximately 11% of *Eucalyptus macrorhyncha* wood samples after MW treatment. No statistically significant reductions in the compressive strength were measured by Kol and Çayir [11] and Hermoso and Vega [40].

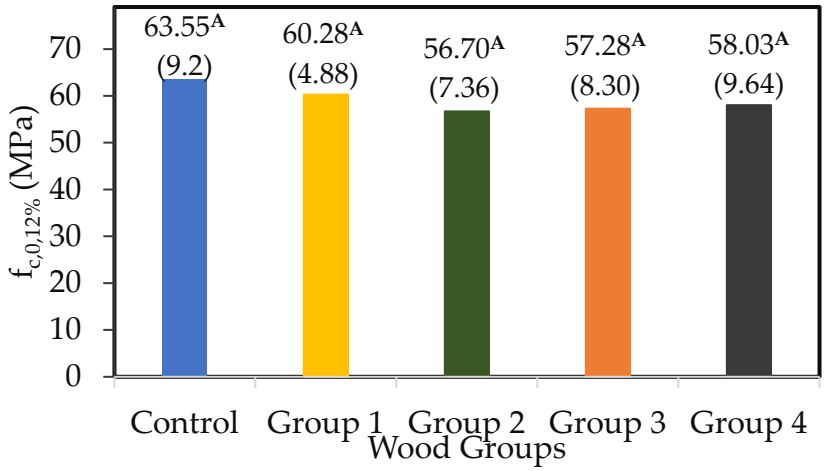

Figure 13. Average compressive strength parallel to the grain of the four wood groups. $f_{c,0,12\%}$ is the compressive strength parallel to the grain at 12% moisture content. The numbers in parentheses are the standard deviation. Values associated with the same letters in Tukey tests do not show significant differences with a *p*-value of 0.05.

Similarly to the WU results, the experimental results of $f_{c,0,12\%}$ also indicated that the IMC of the four wood groups had no statistically significant effects on this mechanical property. These findings are consistent with a previous research work developed by He et al. [54], who MW-dried real-scale wood samples whose IMCs were 40, 60, and 80%. From these results, it is important to note that both the small clean specimens dried in this work and the larger-scale specimens dried by He et al. [54] had a higher IMC than the FSP.

Torgovnikov and Vinden [13] explain that three degrees of MW modification in wood can happen and that a low level of MW modification can enhance the permeability of wood by a factor ranging from 1.1 to 1.5. However, at the same time, it does not have a statistically significant impact on the strength properties of wood, and this may have been the case with the results presented in this work. Hence, given that maritime pine is a commonly used wood species for wooden poles but whose heartwood faces challenges in being impregnated with preservative products [25,58–60], the acceptable results of the compressive strength of MW-dried wood samples and their improved impermeability due to MW drying are favorable points for MW dryings.

Thus, adopting the appropriate parameters of MW drying, such as MW power and drying time, including the MW cycle time in intermittent drying, can lead to minor impacts on the mechanical properties of wood samples since the achieved temperatures will not be so elevated and, consequently, the generated steam pressure.

Finally, even though the results presented in this research came from small specimens, the temperature profiles and moisture behavior presented in this work were similar and supported by other works that used full-scale specimens. Therefore, the outcomes obtained from MW drying small pine specimens not only allow us to infer the effectiveness and relevance of carrying out tests on small specimens, but also serve as a basis for encouraging greater use of MW technology for drying wood.

4. Conclusions

Using small clear heartwood specimens of Portuguese maritime pine to study the temperature profile under MW drying with non-continuous exposition, it was possible to draw the following conclusions:

1. Given the configuration of the MW drying process used in this work, the cooling intervals of 30 s were important to avoid excessive heating, which could result in the burning of some parts of the wood samples.
2. Three stages of temperature behavior were noticed during MW drying, and maximum temperatures were observed in the first few minutes of MW drying.
3. The drying rate comprises three distinct stages: the initial period of liquid movement, followed by a period of constant drying rate, and finally, a period of falling drying rate. A strong positive Pearson's correlation coefficient was identified between the IMC and MW drying time, and strong negative correlations were identified between IMC and average temperature and average temperature and MW drying time.
4. The parameters used in the MW drying of the Portuguese maritime pine samples associated with the cooling intervals provided moisture and temperature behaviors that were effective in increasing the water impregnability of the samples but without generating statistically significant reductions in compressive strength. Additionally, the IMC did not have a statistically significant impact on the water uptake and compressive strength of MW-dried samples.
5. Despite the fact that small clear wood samples of maritime pine were used, the temperature and moisture patterns observed in this study closely matched those of real-scale specimens, which validates the use of small pine samples for testing purposes and demonstrates the positive possibilities of using MW drying in structural-sized wood specimens. Therefore, with adequate MW parameters, it is possible to obtain the benefits of MW without deleterious effects and move from a laboratory to an industrial scale.

Finally, based on the results found here, future research could be carried out in order to investigate, through electron microscopy images, for example, possible changes in the microstructure of the wood, as well as investigations into changes in the porosity and permeability of pine samples. It is also important to indicate that due to the elevated temperatures measured, studies need to be conducted regarding the chemical changes in the MW-dried wood samples. Additionally, based on the results of this work, further tests can be carried out using small clear wood samples or real-scale wood elements.

Author Contributions: Conceptualization, F.J.R.M., R.M.d.S.S., A.M.P.G.D. and A.L.C.; methodology, F.J.R.M. and R.M.d.S.S.; software, F.J.R.M. and A.L.C.; validation, R.M.d.S.S.; formal analysis, F.J.R.M., A.M.P.G.D., A.L.C., R.M.d.S.S. and A.E.P.C.; investigation, F.J.R.M., R.M.d.S.S. and A.E.P.C.; resources, F.J.R.M. and A.M.P.G.D.; writing—original draft preparation, F.J.R.M.; writing—review and editing, F.J.R.M., R.M.d.S.S., A.M.P.G.D. and A.L.C.; supervision, A.M.P.G.D., A.L.C. and R.M.d.S.S.; project administration, A.M.P.G.D.; funding acquisition, F.J.R.M. and A.M.P.G.D. All authors have read and agreed to the published version of the manuscript.

Funding: This work is financed by national funds through the Foundation for Science and Technology—FCT, from Portugal under grant agreement 2021.07636.BD, the FCT, the Ministry of Science, Technology and Higher Education (Portuguese: Ministério da Ciência, Tecnologia e Ensino Superior or MCTES), the Programa Operacional da Região Centro (CENTRO 2020), and the European Social Fund (Portuguese: Fundo Social Europeu or FSE) attributed to the first author (https://doi.org/10.54499/2021.07636.BD). This work was partly financed by FCT/MCTES through national funds (PIDDAC) under the R&D Unit Institute for Sustainability and Innovation in Structural Engineering (ISISE), under reference UIDB/04029/2020 (doi.org/10.54499/UIDB/04029/2020), and under the Associate Laboratory Advanced Production and Intelligent Systems ARISE under reference LA/P/0112/2020.

Data Availability Statement: Data are contained within the article.

Acknowledgments: We are also thankful to the Department of Civil Engineering of the University of Coimbra, the Innovation and Competence Forest Centre—SerQ, and the Department of Chemistry, Unit of Fiber Materials and Environmental Technologies (FibEnTech-UBI), University Beira Interior, for all support provided in the development of this work.

Conflicts of Interest: The authors declare no conflicts of interest.

References

1. Torgovnikov, G.; Vinden, P. MW and RF Applications Case Histories. In Proceedings of the Fourth World Congress on Microwave and Radio Frequency Application, Austin, TX, USA, 7–12 November 2004; pp. 77–78.
2. Mascarenhas, F.J.R.; Dias, A.M.P.G.; Christoforo, A.L. State of the Art of Microwave Treatment of Wood: Literature Review. *Forests* **2021**, *12*, 745. [CrossRef]
3. Torgovnikov, G.; Vinden, P. Microwave Wood Modification Technology and Its Applications. *For. Prod. J.* **2010**, *60*, 173–182. [CrossRef]
4. Engelund, E.T.; Thygesen, L.G.; Svensson, S.; Hill, C.A.S. A Critical Discussion of the Physics of Wood-Water Interactions. *Wood Sci. Technol.* **2013**, *47*, 141–161. [CrossRef]
5. *Forest Products Laboratory Wood Handbook: Wood as an Engineering Material*; General Technical Report FPL-GTR-282; USDA: Washington, DC, USA, 2021; ISBN 1892529025.
6. Metaxas, A.C.; Meredith, R.J. *Industrial Microwave Heating*, 3rd ed.; Short Run Press Ltd.: Exeter, UK, 2008; Volume 24, ISBN 9780906048894.
7. Sahin, H.; Ay, N. Dielectric Properties of Hardwood Species at Microwave Frequencies. *J. Wood Sci.* **2004**, *50*, 375–380. [CrossRef]
8. Oloyede, A.; Groombridge, P. The Influence of Microwave Heating on the Mechanical Properties of Wood. *J. Mater. Process. Technol.* **2000**, *100*, 67–73. [CrossRef]
9. Du, G.; Wang, S.; Cai, Z. Microwave Drying of Wood Strands. *Dry. Technol.* **2005**, *23*, 2421–2436. [CrossRef]
10. Terziev, N.; Daniel, G.; Torgovnikov, G.; Vinden, P. Effect of Microwave Treatment on the Wood Structure of Norway Spruce and Radiata Pine. *Bioresources* **2020**, *15*, 5616–5626. [CrossRef]
11. Kol, H.Ş.; Çayır, B. The Effects of Increasing Preservative Uptake by Microwave Pre-Treatment on the Microstructure and Mechanical Properties of Oriental Spruce Wood. *Wood Mater. Sci. Eng.* **2022**, *18*, 732–738. [CrossRef]
12. Kol, H.Ş.; Çayır, B. Increasing the Impregnability of Oriental Spruce Wood via Microwave Pretreatment. *Bioresources* **2021**, *16*, 2513–2523.
13. Torgovnikov, G.; Vinden, P. High-Intensity Microwave Wood Modification for Increasing Permeability. *For. Prod. J.* **2009**, *59*, 84–92.
14. Xiao, H.; Lin, L.; Fu, F. Temperature Characteristics of Wood during Microwave Treatments. *J. Res.* **2018**, *29*, 1815–1820. [CrossRef]
15. Zielonka, P.; Dolowy, K. Microwave Drying of Spruce: Moisture Content, Temperature, and Heat Energy Distribution. *For. Prod. J.* **1998**, *48*, 77–80.
16. Zielonka, P.; Gierlik, E. Temperature Distribution during Conventional and Microwave Wood Heating. *Holz Als Roh Und Werkst.* **1999**, *57*, 247–249. [CrossRef]
17. Sethy, A.K.; Torgovnikov, G.; Vinden, P.; Przewloka, S. Moisture Conditioning of Wood Using a Continuous Microwave Dryer. *Dry. Technol.* **2016**, *34*, 318–323. [CrossRef]
18. Ouertani, S.; Koubaa, A.; Azzouz, S.; Bahar, R.; Hassini, L.; Belghith, A. Microwave Drying Kinetics of Jack Pine Wood: Determination of Phytosanitary Efficacy, Energy Consumption, and Mechanical Properties. *Eur. J. Wood Wood Prod.* **2018**, *76*, 1101–1111. [CrossRef]
19. Huang, R.; Wu, Y.; Zhao, Y.; Lu, J.; Jiang, J.; Chen, Z. Factors Affecting the Temperature Increasing Rate in Wood during Radio-Frequency Heating. *Dry. Technol.* **2013**, *31*, 246–252. [CrossRef]
20. Ouertani, S.; Hassini, L.; Azzouz, S.; Torres, S.S.; Belghith, A.; Koubaa, A. Modeling of Combined Microwave and Convective Drying of Wood: Prediction of Mechanical Behavior via Internal Gas Pressure. *Dry. Technol.* **2015**, *33*, 1234–1242. [CrossRef]
21. Alonso-Esteban, J.I.; Carocho, M.; Barros, D.; Velho, M.V.; Heleno, S.; Barros, L. Chemical Composition and Industrial Applications of Maritime Pine (*Pinus pinaster* Ait.) Bark and Other Non-Wood Parts. *Rev. Environ. Sci. Bio/Technol.* **2022**, *21*, 583–633. [CrossRef]

22. Meredieu, C.; Brunet, Y.; Danjon, F.; Défossez, P.; Dupont, S.; Kamimura, K.; Gardiner, B. *Pinus pinaster* in Europe: Distribution, Habitat, Usage and Threat. In *European Atlas of Forest Tree Species*; San-Miguel-Ayanz, J., de Rigo, D., Caudullo, G., Houston Durrant, T., Mauri, A., Eds.; Publications Office of the European Union: Luxembourg, 2016; pp. 128–129.
23. Ganguly, S.; Balzano, A.; Petrič, M.; Kržišnik, D.; Tripathi, S. Effects of Different Energy Intensities of Microwave Treatment on Heartwood and Sapwood Microstructures in Norway Spruce. *Forests* **2021**, *12*, 598. [CrossRef]
24. Leggate, W.; Redman, A.; Wood, J.; Bailleres, H.; Lee, D.J. Radial Permeability of the Hybrid Pine (*Pinus elliottii* × *Pinus caribaea*) in Australia. *Bioresources* **2019**, *14*, 4358–4372. [CrossRef]
25. *CEN EN 350*; Durability of Wood and Wood-Based Products—Testing and Classification of the Durability to Biological Agents of Wood and Wood-Based Materials. iTeh Inc.: Brussels, Belgium, 2016.
26. Sedighi-Gilani, M.; Vontobel, P.; Lehmann, E.; Carmeliet, J.; Derome, D. Liquid Uptake in Scots Pine Sapwood and Hardwood Visualized and Quantified by Neutron Radiography. *Mater. Struct./Mater. Constr.* **2014**, *47*, 1083–1096. [CrossRef]
27. Hansmann, C.; Gindl, W.; Wimmer, R.; Teischinger, A. Permeability of Wood—A Review. *Drev. Vysk./Wood Res.* **2002**, *47*, 1–16.
28. *ISO 13061-1*; Physical and Mechanical Properties of Wood—Test Methods for Small Clear Wood Specimens—Part 1: Determination of Moisture Content for Physical and Mechanical Tests. ISO: Geneva, Switzerland, 2014.
29. *BS 373:1957*; Methods of Testing Small Clear Specimens of Timber. BSI: London, UK, 1999.
30. Mascarenhas, F.J.R.; Dias, A.M.P.G.; Christoforo, A.L.; dos Santos Simões, R.M.; Cunha, A.E.P. Effect of Microwave Treatment on Drying and Water Impregnability *Pinus pinaster* and *Eucalyptus globulus*. *Maderas Cienc. Tecnol.* **2023**, *25*, 1–14. [CrossRef]
31. Al-Khuseibi, M.K.; Sablani, S.S.; Perera, C.O. Comparison of Water Blanching and High Hydrostatic Pressure Effects on Drying Kinetics and Quality of Potato. *Dry. Technol.* **2005**, *23*, 2449–2461. [CrossRef]
32. Niemz, P.; Teischinger, A.; Sandberg, D. (Eds.) *Handbook of Wood Science and Technology*; Springer: Cham, Switzerland, 2023.
33. He, Z.; Qian, J.; Qu, L.; Wang, Z.; Yi, S. Simulation of Moisture Transfer during Wood Vacuum Drying. *Results Phys.* **2019**, *12*, 1299–1303. [CrossRef]
34. Benabou, L. Predictions of Compressive Strength and Kink Band Orientation for Wood Species. *Mech. Mater.* **2010**, *42*, 335–343. [CrossRef]
35. Šefc, B.; Trajković, J.; Sinković, T.; Hasan, M.; Ištok, I. Compression Strength of Fir and Beech Wood Modified by Citric Acid. *Drv. Ind.* **2012**, *63*, 45–50. [CrossRef]
36. Aicher, S.; Stapf, G. Compressive Strength Parallel to the Fiber of Spruce with High Moisture Content. *Eur. J. Wood Wood Prod.* **2016**, *74*, 527–542. [CrossRef]
37. Zhao, C.; Liu, D.; Zhang, C.; Li, Y.; Wang, Y. Influence of Specimen Size on the Compressive Strength of Wood. *Buildings* **2024**, *14*, 1156. [CrossRef]
38. *ABNT NBR 7190-1*; Projeto de Estruturas de Madeira Parte 1: Critérios de Dimensionamento. ABNT: Rio de Janeiro, Brazil, 2022.
39. *CEN EN 408*; Timber Structures—Structural Timber and Glued Laminated Timber—Determination of Some Physical and Mechanical Properties. iTeh: Brussels, Belgium, 2012.
40. Hermoso, E.; Vega, A. Effect of Microwave Treatment on the Impregnability and Mechanical Properties of *Eucalyptus globulus* Wood. *Maderas Cienc. Tecnol.* **2016**, *18*, 55–64. [CrossRef]
41. *Software Minitab*, version 18; Minitab: State College, PA, USA, 2018.
42. Weng, X.; Zhou, Y.; Fu, Z.; Gao, X.; Zhou, F.; Jiang, J. Effects of Microwave Pretreatment on Drying of 50 mm-Thickness Chinese Fir Lumber. *J. Wood Sci.* **2021**, *67*, 13. [CrossRef]
43. Leiker, M.; Adamska, M.A. Energy Efficiency and Drying Rates during Vacuum Microwave Drying of Wood. *Holz Als Roh Und Werkst.* **2004**, *62*, 203–208. [CrossRef]
44. Vinden, P.; Torgovnikov, G.; Hann, J. Microwave Modification of Radiata Pine Railway Sleepers for Preservative Treatment. *Eur. J. Wood Wood Prod.* **2011**, *69*, 271–279. [CrossRef]
45. Dashti, H.; Tarmian, A.; Faezipour, M.; Hedjazi, S.; Shahverdi, M. Mass Transfer Through Microwave-Treated Fir Wood (*Abies alba* L.): A Gymnosperm Species with Torus Margo Pit Membrane. *Dry. Technol.* **2013**, *31*, 359–364. [CrossRef]
46. Hansson, L.; Antti, L. Modeling Microwave Heating and Moisture Redistribution in Wood. *Dry. Technol.* **2008**, *26*, 552–559. [CrossRef]
47. Vongpradubchai, S.; Rattanadecho, P. The Microwave Processing of Wood Using a Continuous Microwave Belt Drier. *Chem. Eng. Process. Process Intensif.* **2009**, *48*, 997–1003. [CrossRef]
48. Zhang, Y.; Jia, K.; Cai, L.; Shi, S.Q. Acceleration of Moisture Migration in Larch Wood Through Microwave Pre-Treatments. *Dry. Technol.* **2013**, *31*, 666–671. [CrossRef]
49. Petty, J.A.; Preston, R.D. Permeability and Structure of the Wood of Sitka Spruce. *Proc. R. Soc. B Biol. Sci.* **1970**, *175*, 149–166. [CrossRef]
50. Koubaa, A.; Perré, P.; Hutcheon, R.; Lessard, J. Complex Dielectric Properties of the Sapwood of Aspen, White Birch, Yellow Birch, and Sugar Maple. *Dry. Technol.* **2008**, *26*, 568–578. [CrossRef]
51. Antti, A.L.; Perre, P. A Microwave Applicator for on Line Wood Drying: Temperature and Moisture Distribution in Wood. *Wood Sci. Technol.* **1999**, *33*, 123–138. [CrossRef]
52. Henry, F.; Gaudillat, M.; Costa, L.C.; Lakkis, F. Free and/or Bound Water by Dielectric Measurements. *Food Chem.* **2003**, *82*, 29–34. [CrossRef]

53. Laboratório Nacional de Engenharia Civil (LNEC). *Ficha M9—Madeira Para Construção: Humidade Da Madeira [Wood for Construction: Wood Moisture]*; LNEC: Lisbon, Portugal, 1997.
54. He, S.; Lin, L.; Fu, F.; Zhou, Y.; Fan, M. Microwave Treatment for Enhancing the Liquid Permeability of Chinese Fir. *Bioresources* **2014**, *9*, 1914–1923. [CrossRef]
55. Wang, Z.; Xu, E.; Fu, F.; Lin, L.; Yi, S. Industrial Crops & Products Characterization of Wood Cell Walls Treated by High-Intensity Microwaves: Effects on Physicochemical Structures and Micromechanical Properties. *Ind. Crop. Prod.* **2022**, *187*, 115341. [CrossRef]
56. Machado, J.S. Effect of Microwave Treatment on Oak Compression Strength. *Silva Lusit* **2006**, *14*, 51–58.
57. Balboni, B.M.; Ozarska, B.; Garcia, J.N.; Torgovnikov, G. Microwave Treatment of *Eucalyptus macrorhyncha* Timber for Reducing Drying Defects and Its Impact on Physical and Mechanical Wood Properties. *Eur. J. Wood Wood Prod.* **2018**, *76*, 861–870. [CrossRef]
58. Dias, A.M.A.; Santos, P.G.G.; Dias, A.M.P.G.; Silvestre, J.D.; de Brito, J. Life Cycle Assessment of a Preservative Treated Wooden Deck. *Wood Mater. Sci. Eng.* **2022**, *17*, 502–512. [CrossRef]
59. Morgado, T.F.M.; Rodrigues, J.; Machado, J.S.; Dias, A.M.P.G.; Cruz, H. Bending and Compression Strength of Portuguese Maritime Pine Small-Diameter Poles. *For. Prod. J.* **2009**, *59*, 23–28.
60. Morgado, T.F.M.; Dias, A.M.P.G.; Machado, J.S.; Negrão, J.H.; Marques, A.F.S. Grading of Portuguese Maritime Pine Small-Diameter Roundwood. *J. Mater. Civ. Eng.* **2017**, *29*, 04016209. [CrossRef]

Disclaimer/Publisher's Note: The statements, opinions and data contained in all publications are solely those of the individual author(s) and contributor(s) and not of MDPI and/or the editor(s). MDPI and/or the editor(s) disclaim responsibility for any injury to people or property resulting from any ideas, methods, instructions or products referred to in the content.